VII International Conference on Textile Composites and Inflatable Structures
STRUCTURAL MEMBRANES 2015
E. Oñate, K.-U.Bletzinger and B. Kröplin (Eds)

ELASTO-VISCOPLASTIC MATERIAL MODEL CONSIDERING LARGE STRAINS FOR ETFE-FOILS

MARIANNA COELHO* AND DEANE ROEHL†

* Universidade do Estado de Santa Catarina
Department of Civil Engineering
Rua Paulo Malschitzki, 200, 89219-710, Joinville, SC, Brazil
e-mail: marianna.lorencet@udesc.br

† Pontificia Universidade Catolica do Rio de Janeiro
Department of Civil Engineering
Rua Marques de Sao Vicente 225, 22451-900 Rio de Janeiro, Brazil
Email: droehl@puc-rio.br

Key words: Elasto-viscoplastic material, Inflatable structures, ETFE-Foils, Large strains

Abstract. The growing use of ETFE-Foils in pneumatic structures has motivated the research in material models for thermoplastic polymeric. This type of polymer is more resistant to solvents and other chemicals. The lightweight of the ETFE foil is one of the most important features that motivates its use in structural buildings. Moreover, it has been applied often to roofs, resulting in low costs for the foundation. The translucency property is advantageous, because it allows the utilization of natural light, reducing the use of artificial light. Another property related with resource consumption is the anti-adhesive nature of ETFE. This property means that roofs and atria need to be cleaned less frequently, leading to a reduction in the cost of the building maintenance.

ETFE membrane structures clearly present large deformations by which the small strain material model fails to give good results. Beyond this behavior some experiments showed the dependency of the ETFE mechanical properties with temperature. These experiments indicated viscoplastic material behavior, characterized by different responses for different strain rates / load rates and different temperatures.

The present work shows an implementation in a finite element software of an elasto-viscoplastic material model considering large strains for the ETFE membranes. The parameters were obtained with uniaxial experiments analysis from literature. The results of the numerical model show good agreement with the experiments.

1 Introduction

ETFE(Ethylene tetrafluoroethylene) is a polymer classified as a semi-crystalline thermoplastic. This type of polymer is more resistant to solvents and other chemicals than others.

The low weight of ETFE is one of the most important features that motivates the use of this material in structural buildings. Moreover, it has been used more often on roofs, resulting in a lower cost for the foundation.

The translucent property is advantageous, because it allows the utilization of natural light, reducing the energy consumption. Another property related to resource consumption and commented by Robinson-Gayle et al. [9] is the anti-adhesive nature of ETFE. This property means that roofs and atria need to be cleaned less frequently reducing maintenance cost.

Moritz [8] and Hu [4] performed some experiments in ETFE for different temperatures. They observed that the ETFE properties change significantly with temperature change.

The elasto-viscoplastic material model reflects the plastic deformation dependence with time. The temperature is often related with this phenomena.

According to Souza Neto et al. [14], materials such as metals, rubbers, geomaterials in general, concrete and composites may all present substantial time-dependent mechanical behavior.

The phenomenological aspects for elasto-viscoplasticity are: strain rate dependence, creep and relaxation.

The strain rate dependence is observed when a material is subjected to tests carried out under different prescribed strain rates. According to Souza Neto et al. [14], the elasticity modulus is mostly independent of the rate of loading but, the initial yield limit as well as the hardening curve depend strongly on the rate of straining. This rate-dependence is also observed at low temperatures, but usually becomes significant only at higher temperatures.

Creep is the phenomenon by which that at a constant stress condition the strain increases. For different levels of stress the response for strain is also different.

Relaxation occurs when by a constant strain stress decays in time.

The present work aims to model this ETFE characteristics using an elasto-viscoplastic material model considering large strains.

2 Material modeling

ETFE–foils behave as membranes, therefore the analyses were carried out considering plane stress state.

The deformation gradient $\mathbf{F}$ transforms the reference configuration into the actual configuration.

$$\mathbf{F} = \frac{\partial \mathbf{x}}{\partial \mathbf{X}} \tag{1}$$

where $\mathbf{x}$ is the position of a point in current configuration and $\mathbf{X}$ is the position of a point in the reference configuration.

The multiplicative decomposition of the deformation gradient $\mathbf{F}$ is the main hypothesis in the finite strain elastoplasticity [7]. According to Lee and Liu [7], the combination of elastic and plastic strains, both finite, calls for a more careful study of the kinematics than the usual assumption that the total strain components are simply the sum of the elastic and plastic components, as it is assumed in the infinitesimal strain theory.

$$\mathbf{F} = \mathbf{F}^{e}\mathbf{F}^{vp} \tag{2}$$

The Lagrangian description was used in the implementation, therefore the strain and stress tensors will be defined in this description.

The Green-Lagrange strain tensor is defined by:

$$\mathbf{E} = \frac{1}{2}\left(\mathbf{F}^{T}\mathbf{F} - \mathbf{I}\right) \tag{3}$$

The logarithmic strain measure is computed as:

$$\mathbf{E}_{L} = ln(\mathbf{U}) \tag{4}$$

where $\mathbf{U}$ is termed the right stretch tensor.

$$\mathbf{U} = \sqrt{\mathbf{C}} \tag{5}$$

where $\mathbf{C}$ is the right Cauchy-Green tensor and its spectral representation is given by:

$$\mathbf{C} = \mathbf{F}^{T}\mathbf{F} = \mathbf{U}^{2} = \sum_{i=0}^{m} \lambda_{i}\mathbf{M}_{i} \qquad i = 1, 2 \tag{6}$$

where λ_i are the principal stretches and $\mathbf{M}_i$ are the eigenprojections.

The conjugated stress pair with Green-Lagrange strain tensor is the second Piola-Kirchhoff stress tensor($\mathbf{S}$).

The conjugated stress pair with logarithmic strain tensor is the Kirchhoff stress tensor. The Kirchhoff trial stress is calculated with the elastic constitutive material tensor for small strains ($\mathbf{D}$):

$$\mathbf{T}_{n+1}^{e^{trial}} = \mathbf{D}\mathbf{E}_{L}{}_{n+1}^{e^{trial}} \tag{7}$$

$$\mathbf{D} = \frac{E}{1-\nu^{2}} \begin{bmatrix} 1 & \nu & 0 \\ \nu & 1 & 0 \\ 0 & 0 & \frac{1-\nu}{2} \end{bmatrix} \tag{8}$$

where ν is the Poisson ratio and E is the elastic modulus.

2.1 Von Mises yield criteria - Plane Stress

Figure 1 presents the experimental data from uniaxial and biaxial test of ETFE from works of Moritz [8], Galliot and Luchsinger [3], and DuPONT^{TM} Tefzel® [2] and an adjusted von Mises yield curve. This yield surface was generated considering an yield stress of $16MPa$. Figure 1 shows that the von Mises criteria is a good approximation for the experimental data for the ETFE material.

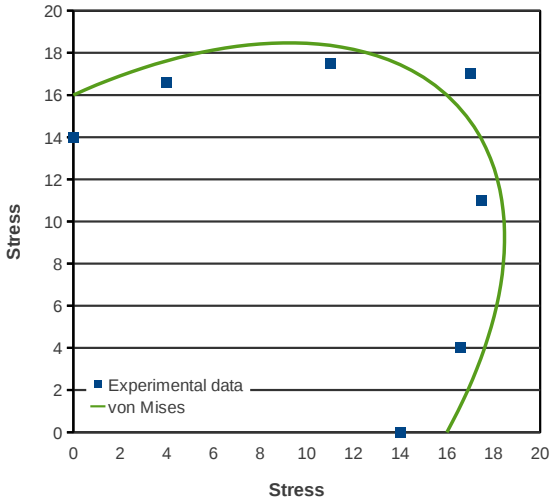

Figure 1: Experimental data from uniaxial and biaxial test of ETFE and adjusted von Mises yield curve

The von Mises yield criteria postulates that yielding begins when $J2$, the second invariant of the deviatoric stress, reaches a critical value (k) [15]:

$$f(J2) = \sqrt{J2} - k = 0 \quad \leftrightarrow \quad f(J2) = J2 - k^2 = 0 \tag{9}$$

In vector notation the deviatoric stress $\mathbf{s}$ is written:

$$\mathbf{s} = [s_{11} \ s_{22} \ s_{12}] \tag{10}$$

which can be obtained by the projection of the stress tensor on the deviatoric plane.

$$\mathbf{s} = dev[\mathbf{S}] = \bar{\mathbf{P}}\mathbf{S} \qquad \bar{\mathbf{P}} = \frac{1}{3}\begin{bmatrix} 2 & -1 & 0 \\ -1 & 2 & 0 \\ 0 & 0 & 3 \end{bmatrix} \tag{11}$$

$J2$ is calculated through:

$$J2 = \mathbf{SPS} \tag{12}$$

Similarly the elastic and plastic strain tensors ($\mathbf{E}^e$, $\mathbf{E}^p$) are collected in vector form as:

$$\mathbf{E}^e = [E^e_{11}\ E^e_{22}\ 2E^e_{12}] \qquad \mathbf{E}^p = [E^p_{11}\ E^p_{22}\ 2E^p_{12}]$$

and the deviatoric strain is given by:

$$\mathbf{e} = dev[\mathbf{E}] = \mathbf{P}\mathbf{E} \qquad \mathbf{P} = \frac{1}{3}\begin{bmatrix} 2 & -1 & 0 \\ -1 & 2 & 0 \\ 0 & 0 & 6 \end{bmatrix} \tag{13}$$

Linear isotropic hardening is considered, for which the scalar hardening state variable is:

$$q = \sigma_y + K\alpha \tag{14}$$

where α is the amount of plastic flow.

2.2 Small strain elasto-viscoplasticity

The formulation used for the elasto-viscoplastic material is classic and it is presented for instance in the studies of Simo and Taylor [13], Simo and Hughes [12], and Souza Neto et al.[14].

The total strain $\mathbf{E}$ splits into a elastic strain $\mathbf{E}^e$ and a plastic strain $\mathbf{E}^p$:

$$\mathbf{E} = \mathbf{E}^e + \mathbf{E}^{vp} \tag{15}$$

The elastic constitutive law considering linear elasticity is given by the relation:

$$\dot{\mathbf{S}} = \mathbf{D} : (\dot{\mathbf{E}} - \dot{\mathbf{E}^{vp}}) \tag{16}$$

The yield condition ($f(\mathbf{S}, q)$) is given by equation 9.

The flow rule and the hardening law in associative plasticity models are given respectively by:

$$\dot{\boldsymbol{E}_{\boldsymbol{vp}}} = \gamma\frac{\partial f}{\partial \mathbf{S}} \tag{17}$$

$$\dot{\boldsymbol{\alpha}} = \gamma\frac{\partial f}{\partial q} \tag{18}$$

where γ is the consistency parameter, $\frac{\partial f}{\partial \mathbf{S}}$ is a function that defines the direction of plastic flow, and $\frac{\partial f}{\partial q}$ is a function that describes the hardening evolution.

The explicit function for γ models describes how the rate of plastic straining varies with the level of stress. There are many models to describe γ. Souza Neto et al. [14] reports that a particular choice should be dictated by its ability to model the dependence of the plastic strain rate on the state of stress for the material under consideration.

The model used in the present work to describe the viscoplastic strain is the Perić Model (apud Souza Neto et al. [14]):

2.2.1 Perić Model

This model is given by:

$$< f_{n+1} >= \begin{cases} \left[\left(\frac{J2(S)}{q}\right)^{1/\epsilon} - 1\right] & if \quad f(S,\sigma_y) \geq 0 \\ 0 & if \quad f(S,\sigma_y) < 0 \end{cases} \tag{19}$$

Modifying $\Delta\gamma$ to include the time parameter the following expression is obtained:

$$\Delta\gamma = \Delta t \cdot \gamma =< f_{n+1} > \frac{\Delta t}{\mu}, \qquad \mu \in (0,\infty) \tag{20}$$

where Δt is time increment.

In the present work the Perić model is used to describe $< f_{n+1} >$ (equation 19). This equation was rewritten in a more stable form, according to Perić apud Souza Neto et al. [14] as:

$$\phi(\Delta\gamma) = \left(\frac{\Delta t}{\Delta\gamma\mu + \Delta t}\right)^{\epsilon} \cdot \left(\frac{1}{2}\bar{f}^2\right) - \frac{1}{3}R^2 = 0 \tag{21}$$

The actual state $(\mathbf{S}, q)$ of stress and hardening force is a solution to the following constrained optimization problem:

$$\begin{aligned} maximise \quad & \mathbf{S} : \dot{\mathbf{E}} - q \cdot \dot{\alpha} \\ subject\ to \quad & f(\mathbf{S}, q) \leq 0 \end{aligned} \tag{22}$$

Solution for the problem 22 satisfies the Kuhn-Tucker optimality conditions, the so called loading/unloading condition.

$$\gamma \geq 0, \qquad f(\mathbf{S}, q) \leq 0, \qquad \gamma f(\mathbf{S}, q) = 0 \tag{23}$$

The updating scheme for integration of the corresponding rate constitutive equations requires the formulation of a numerical algorithm. The implicit Euler or backward scheme is used to discretize the incremental constitutive problem.

The return mapping used in the present work is the closest point projection (Simo and Hughes [12]). This return mapping considers a two-step algorithm called the elastic predictor/plastic corrector algorithm. This algorithm assumes that the first step is elastic, which is called as the elastic trial solution ($\mathbf{S}_{n+1}^{trial}$). If this elastic trial stress violates the yield function a new solution must be obtained with the plastic corrector step. The plastic corrector step and the implementation of the return mapping are detailed in [1]. The plastic multiplier ($\Delta\gamma$) is solved using the Newton-Raphson procedure because of the nonlinear equations in $\Delta\gamma$.

2.3 Large strains

The implementation was carried out in this study preserving the return mapping schemes of the infinitesimal theory presented in section 2.2. Simo [11] showed that using Kirchhoff stress and logarithmic strain, the return mapping algorithm takes a format identical to the standard return mapping algorithms for the infinitesimal theory.

The numerical integration of the elastoplastic model is carried out with the elastic predictor and the plastic corrector scheme. The elastic predictor is calculated based on the multiplicative decomposition presented in equation 2 considering $\mathbf{F}^p_{n+1} = \mathbf{F}^p_n$, the trial elastic deformation gradient is given by:

$$\mathbf{F}^{e^{trial}}_{n+1} = \mathbf{F}_{n+1}\mathbf{F}^{p^{-1}}_{n+1} \tag{24}$$

$$\mathbf{T}^{e^{trial}}_{n+1} = \mathbf{D}\mathbf{E}_{L}{}^{e^{trial}}_{n+1} \tag{25}$$

With the Kirchhoff trial stress the plastic corrector is calculated with the algorithm for small strains, the Kirchhoff stress $\mathbf{T}_{n+1}$ and the plastic deformation gradient $\mathbf{F}^p_{n+1}$ are updated. Finally the consistent elastoplastic tangent moduli is computed.

Simo [10] and Ibrahimbegović ([5],[6]) computed the elastoplastic tangent moduli in spatial description. In the present work the elastoplastic tangent moduli is considered in material description.

The consistent elastoplastic tangent moduli $\frac{d\mathbf{S}}{d\mathbf{E}}$ is computed from the following equation:

$$\mathbf{S} = \mathbf{F}^{-1}\boldsymbol{\tau}\mathbf{F}^{-T} = \mathbf{F}^{-1}\mathbf{R}^{-T}\boldsymbol{\tau}\mathbf{R}^{-1}\mathbf{F}^{-T} \tag{26}$$

After some rearrangement and the consideration of symmetric tensor property $\mathbf{U} = \mathbf{U}^T$, equation 26 is rewritten:

$$\mathbf{S} = \mathbf{U}^{-1}\mathbf{T}\mathbf{U}^{-1} \tag{27}$$

The forth-order tensor $\frac{d\mathbf{S}}{d\mathbf{E}}$ can be written as:

$$\frac{d\mathbf{S}}{d\mathbf{E}} = \frac{d\mathbf{S}}{d\mathbf{C}}\frac{d\mathbf{C}}{d\mathbf{E}} = 2\frac{d\mathbf{S}}{d\mathbf{C}} \qquad\qquad \mathbf{E} = \frac{1}{2}\left(\mathbf{C} - \mathbf{I}\right) \tag{28}$$

The derivative of equation 27 w.r.t $\mathbf{C}$ is given by:

$$2\frac{d\mathbf{S}}{d\mathbf{C}} = 2\left(\frac{\partial\mathbf{U}^{-1}}{\partial\mathbf{C}}\mathbf{T}\mathbf{U}^{-1} + \mathbf{U}^{-1}\frac{\partial\mathbf{T}}{\partial\mathbf{C}}\mathbf{U}^{-1} + \mathbf{U}^{-1}\mathbf{T}\frac{\partial\mathbf{U}^{-1}}{\partial\mathbf{C}}\right) \tag{29}$$

3 Example

Moritz [8] carried out biaxial experiments in the proportion of 3:1 for different levels of temperature (0 °C,+23°C and +35°C). The material is the ASAHI®FLUON ETFE NJ (thickness = 250μm).

These experimental results are compared with the numerical analysis considering elasto-viscoplastic material behavior with large strains.

The mesh used for the numerical analysis is a rectangular membrane presented in figure 2. This mesh has 441 nodes and 400 quadrilateral linear elements. In figure 2 are presented the boundary conditions and the applied loads for this model. The material properties are presented in table 1. The von Mises yield criteria is used in the elasto-viscoplastic model.

The analysis is carried out with the load control.

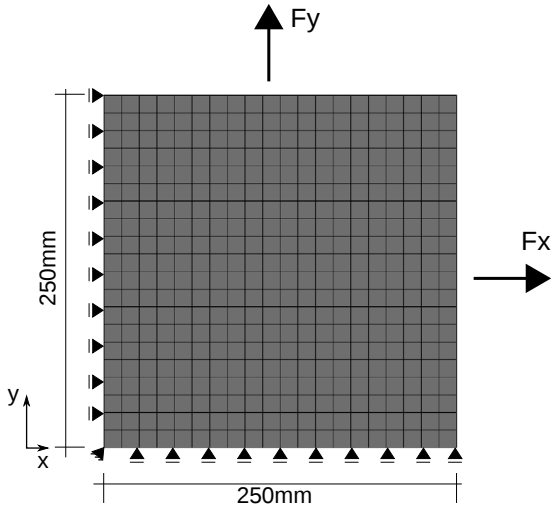

Figure 2: Mesh, geometry and boundary conditions for the biaxial test

Table 1: Material properties of ETFE–foils

Young's modulus (E)	1000MPa
Poisson ratio (ν)	0.43
Yield stress (σ_{y_1})	8.5MPa
Hardening modulus (K_1)	90MPa

As the temperature increases, the viscosity (μ) increases and the rate sensitivity (ϵ) decreases. The values used in the present analysis are shown in table 2

Table 2: Viscosity and rate sensitivity values for ETFE

Temperature (°C)	Viscosity (s)	Rate sensitivity
0	500	10.2
23	1000	2.2
35	2000	0.2

3.1 Results

The results comparing the experimental tests and the numerical analysis are shown in figure 3. These figures show the results for both axis of the biaxial analysis.

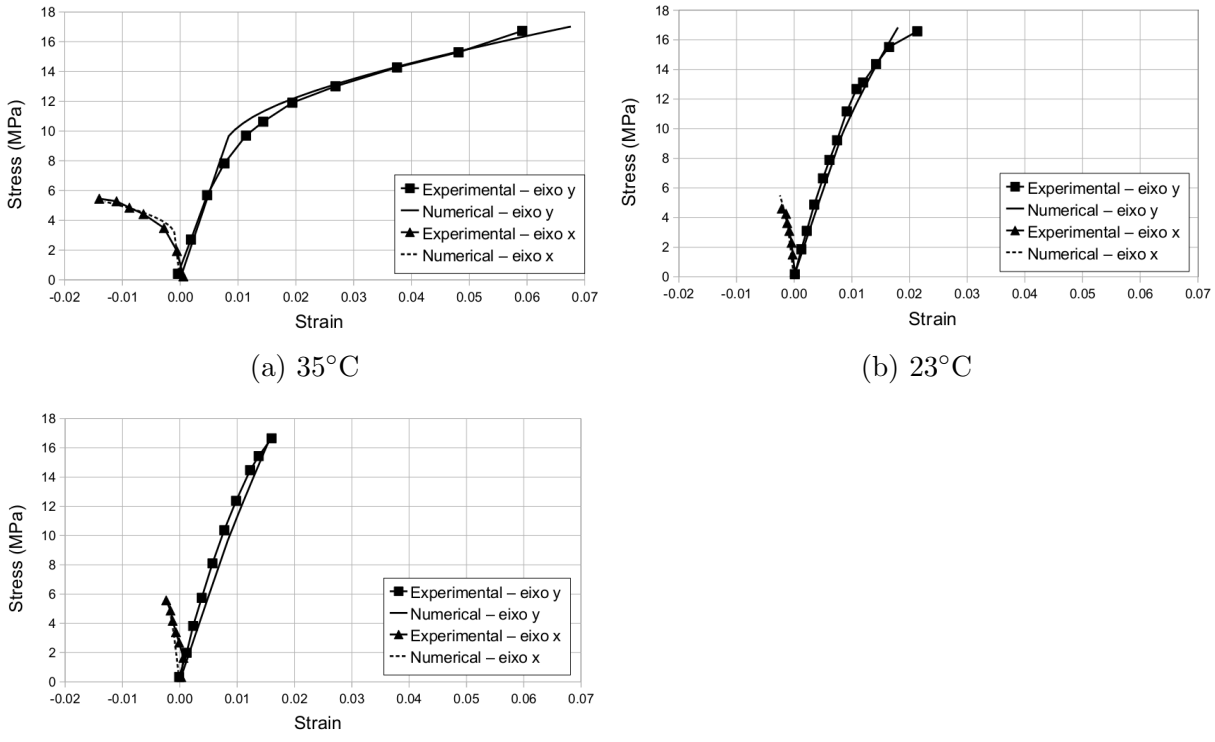

(a) 35°C

(b) 23°C

(c) 0°C

Figure 3: Stress versus strain results for different temperature values.

4 Conclusions

Experimental tests show the dependency of mechanical properties of ETFE with temperature. The strain rate dependence is also observed for ETFE. These characteristics are found in a material with elasto-viscoplastic behavior. In this work an elasto-viscoplastic

material model was implemented in a finite element research software. An example comparing the experimental tests with numerical analysis was performed. The results show good agreement with the experimental results. We conclude that this material model is a good alternative to model ETFE–Foils considering temperature change.

REFERENCES

[1] Marianna A. O. Coelho. *Analysis of pneumatic structures considering nonlinear material models and pressure-volume couppling*. PhD thesis, Pontificia Universidade Catolica do Rio de Janeiro, July 2012.

[2] DuPont Fluoroproducts. *DuPont^{TM} Tefzel© fluorpolymer resin - Properties Handbook*.

[3] C. Galliot and R. H. Luchsinger. Uniaxial and biaxial mechanical properties of ETFE foils. *Polymer Testing*, 30:356–365, 2011.

[4] Jianhui Hu, Wujun Chen, Bing Zhao, and Kai Wang. Uniaxial tensile mechanical properties and model parameters determination of ethylene tetrafluoroethylene (ETFE) foils. *Construction and Building Materials*, 75(0):200–207, 2015.

[5] Adnan Ibrahimbegović. Finite elastoplastic deformation of space-curved membranes. *Computer methods in applied mechanics and engineering*, 119:371–394, 1994.

[6] Adnan Ibrahimbegović. Finite elastoplastic defomation of membrane shells. *Engineering Computations*, 13:122–142, 1996.

[7] E. H. Lee and D. T. Liu. Finite-strain elastic-plastic theory with application to plane-wave analysis. *Journal of applied physics*, 38:19–27, 1967.

[8] Karsten Moritz. *ETFE-Folie als Tragelement*. PhD thesis, Technische Universität München, 2007.

[9] S. Robinson-Gayle, M. Kolokotroni, A. Cripps, and S. Tanno. ETFE foil cushions in roofs and atria. *Construction and Building Materials*, 15:323–327, 2001.

[10] J. C. Simo. A framework for finite strain elastoplasticity based on maximum plastic dissipation and the multiplicative decomposition. Part II: Computational aspects. *Computer Methods in Applied Mechanics and Engineering*, 68:1–31, 1988.

[11] J. C. Simo. Algorithms for static and dynamic multiplicative plasticity that preserve the classical return mapping schemes of the infinitesimal theory. *Computer Methods in Applied Mechanics and Engineering*, 99:61–112, 1992.

[12] J.C. Simo and T.J.R. Hughes. *Computational inelasticity*, volume 7. Springer Verlag, 1998.

[13] J.C. Simo and R.L. Taylor. A return mapping algorithm for plane stress elastoplasticity. *International Journal for Numerical Methods in Engineering*, 22(3):649–670, 1986.

[14] E.A. Souza Neto, D. Perić, and D.R.J. Owen. *Computational methods for plasticity: theory and applications*. Wiley, 2008.

[15] R. von Mises. Mechanik der festen Körper im plastisch- deformablen Zustand. *Nachrichten von der Gesellschaft der Wissenschaften zu Göttingen, Mathematisch-Physikalische Klasse*, 1913:582–592, 1913.